

Supporting Information

Room-Temperature White and Color-Tunable Afterglow by Manipulating Multi-Mode Triplet Emissions

Jianwei Liu,^a Zhimin Ma,^b Zewei Li,^c Yan Liu,^a Xiaohua Fu,^a Hong Jiang,^c Zhiyong Ma^{a*} and Xinru Jia^c

[a] Prof. Z.Y. Ma, Mr. J.W. Liu, Miss Y. Liu, Mr. Xiaohua Fu

Beijing Advanced Innovation Center for Soft Matter Science and Engineering, State Key Laboratory of Organic-Inorganic Composites, College of Chemical Engineering, Beijing University of Chemical Technology, Beijing 100029, China. E-mail:
mazhy@mail.buct.edu.cn.

[b] Dr. Z.M. Ma

National high-tech industrial development zone in Jingdezhen, Jingdezhen, 333000, China.

[c] Prof. X.R. Jia, Prof. H. Jiang, Mr. Z.W. Li

Beijing National Laboratory for Molecular Sciences, Key Laboratory of Polymer Chemistry and Physics of the Ministry of Education, College of Chemistry and Molecular Engineering, Peking University, Beijing 100871, China.

Jianwei Liu and Zhimin Ma contributed equally.

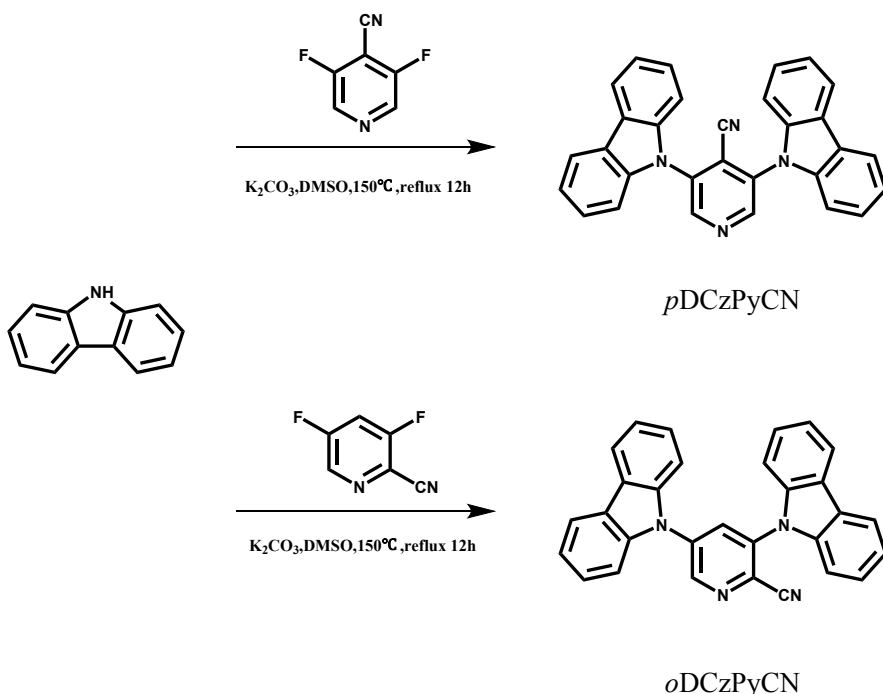
1. Materials and General Methods

All the solvents and reactants were purchased from commercialized companies and used as received without further purification except for specifying otherwise.

^1H NMR was recorded on the 400 MHz (Bruker ARX400) and ^{13}C NMR spectra were recorded on the Bruker 125 MHz spectrometer at room temperature with DMSO and CDCl_3 as the solvent and tetramethylsilane (TMS) as the internal standard. ESI high resolution mass-spectra (HRMS) were acquired on a Bruker Apex IV FTMS mass spectrometer. Transient and delayed photoluminescence spectra were performed on the Hitachi F-4600 or Edinburgh Instruments FLS980 fluorescence spectrophotometer. Luminescence lifetime were acquired on the Edinburgh Instruments FLS980 fluorescence spectrophotometer ($\lambda_{\text{ex}}=365$ nm). Single crystal X-ray diffraction data were collected with a NONIUS KappaCCD diffractometer with graphite monochromator and Mo $\text{K}\alpha$ radiation [$\lambda(\text{MoK}\alpha)=0.71073$ Å]. Structures were solved by direct methods with SHELXS-97 and refined against F2 with SHELXS-97.

TD-DFT calculations were conducted on Gaussian 09 program with a method similar to previous literature.^[1] Ground state (S_0) geometries of *p*DCzPyCN, *o*DCzPyCN were directly selected from single crystal structures and were used as molecular models without further optimization. On the basis of this, exciton energies in singlet (S_n) and triplet states (T_n) were estimated through a combination of TDDFT and B3LYP at the 6-311+G(d, p) level. Kohn-Sham frontier orbital analysis was subsequently performed based on the results of theoretical calculation to elucidate the mechanisms of possible singlet-triplet intersystem crossings, in which the channels from S_1 to T_n are believed to share part of the same transition orbital compositions. Herein, energy levels of the possible T_n states are considered to lie within the range of $ES_1 \pm 0.3$ eV.^[2] $E_{TD}=E(T_1)-E(T_1^*)$, where $E(T_1)$ is the energy level of T_1 calculated from the monomer and $E(T_1^*)$ is the energy level of T_1^* calculated from the dimer.

2. Synthesis of targeted molecule *p*DCzPyCN, *o*DCzPyCN



Scheme S1. The synthetic routes to prepare *p*DCzPyCN, *o*DCzPyCN.

***p*DCzPyCN:** 4-Cyano-3,5-difluoropyridine (610.5 mg, 5 mmol), Carbazole (1.672 g, 10 mmol), K_2CO_3 (2.075 g, 15 mmol) were added to a 100 mL round-bottomed flask. Then DMSO (20 mL, AR grade) was added to the flask. The mixed solution was refluxed at 150 °C for 12h. After the reaction was over, the resultant mixture was cooled down to room temperature and washed with water. Then the reaction mixture was extracted with CH_2Cl_2 (3×30 mL) and the organic layers were collected and dried with anhydrous Na_2SO_4 . After removing the solvent by vacuum-rotary evaporation, the solid residue was purified by column chromatography (silica gel, 10:1 v/v, PE/ CH_2Cl_2). Yield: 0.35 g of green powder (16.12%).

^1H NMR (400 MHz, Chloroform-*d*) δ 9.10 (s, 2H), 8.19 (d, $J = 7.9$ Hz, 4H), 7.53 (ddd, $J = 8.4, 7.3, 1.2$ Hz, 4H), 7.44 – 7.33 (m, 8H).

^{13}C NMR (101 MHz, Chloroform-d) δ 149.49, 140.33, 137.02, 126.75, 124.47, 121.84, 120.98, 109.46.

HR-ESI-MS Calcd. For $\text{C}_{30}\text{H}_{19}\text{N}_4$ [$\text{M}+\text{H}]^+$: 435.160423. Found: 435.160463.

***o*DCzPyCN:** *o*DCzPyCN was prepared under the identical synthetic conditions described in the preparation of *p*DCzPyCN. Yield: 0.14 g of white powder (18.43%).

¹H NMR (400 MHz, Chloroform-*d*) δ 9.22 (d, *J* = 2.3 Hz, 1H), 8.26 (d, *J* = 2.3 Hz, 1H), 8.16 (dd, *J* = 11.7, 7.7 Hz, 4H), 7.59 – 7.44 (m, 6H), 7.44 – 7.33 (m, 6H).

¹³C NMR (101 MHz, DMSO-d6) δ 149.12, 140.80, 139.91, 139.43, 139.10, 135.88, 129.96, 127.20, 127.10, 124.12, 123.86, 121.96, 121.62, 121.20, 121.16, 115.97, 110.75, 110.64.

HR-ESI-MS Calcd. For C₃₀H₁₉N₄ [M+H]⁺: 435.160423. Found: 435.160367.

3. NMR spectra and HR-MS of *p*DCzPyCN, *o*DCzPyCN.

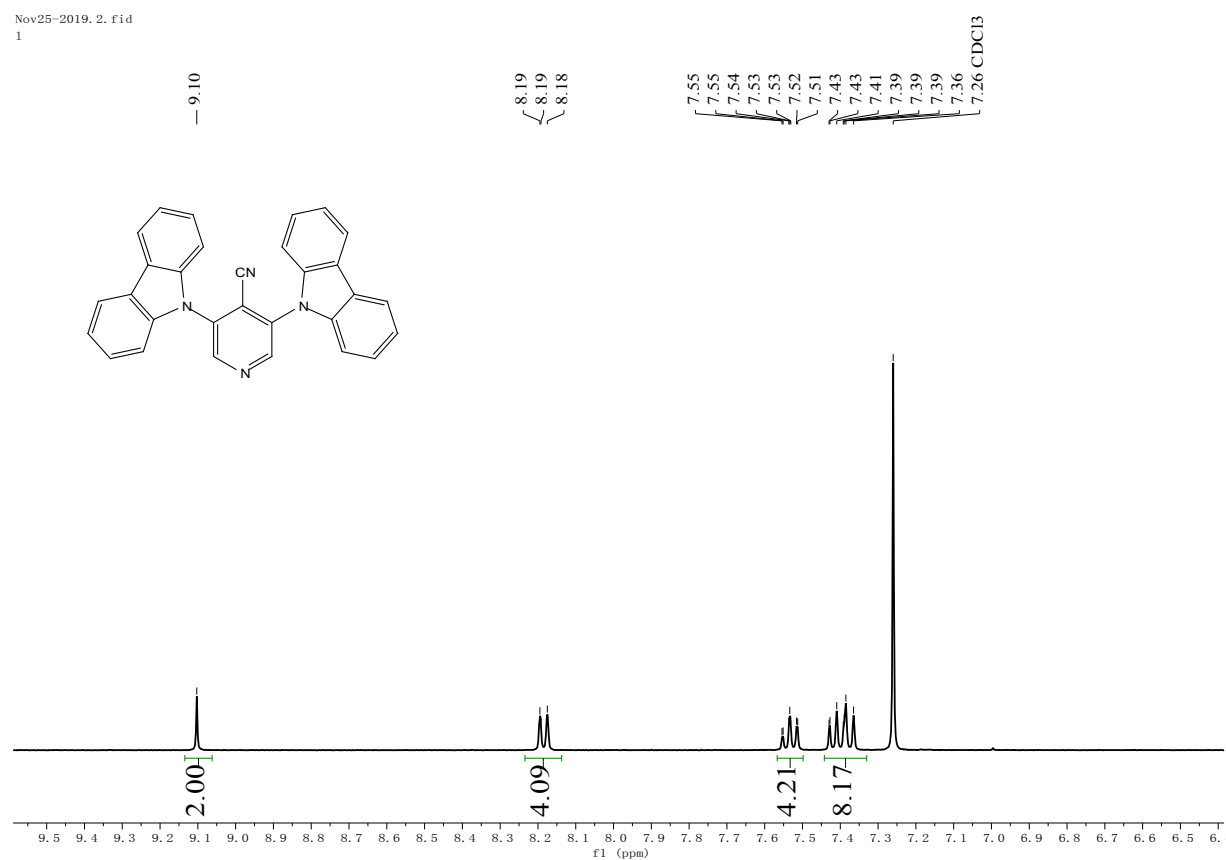


Figure S1. ¹H NMR spectrum of *p*DCzPyCN in CDCl₃.

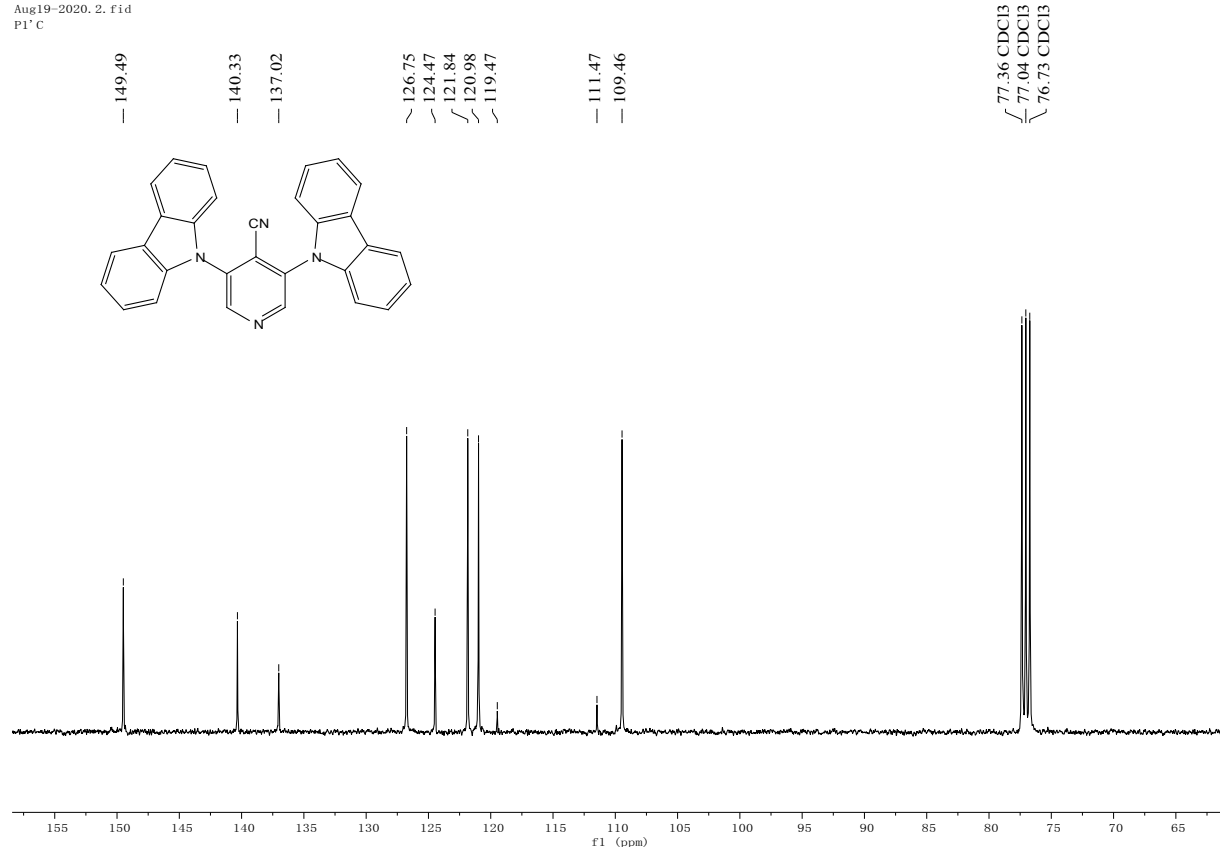


Figure S2. ^{13}C NMR spectrum of *p*DCzPyCN in CDCl_3 .

Peking University Mass Spectrometry Sample Analysis Report

Analysis Info

Analysis Name FTMS-20080215_Pos_20200828_000002.d
Sample pDCzPyCN
Comment

Acquisition Date 8/28/2020 2:30:57 PM
Instrument Bruker Solarix XR FTMS
Operator Peking University

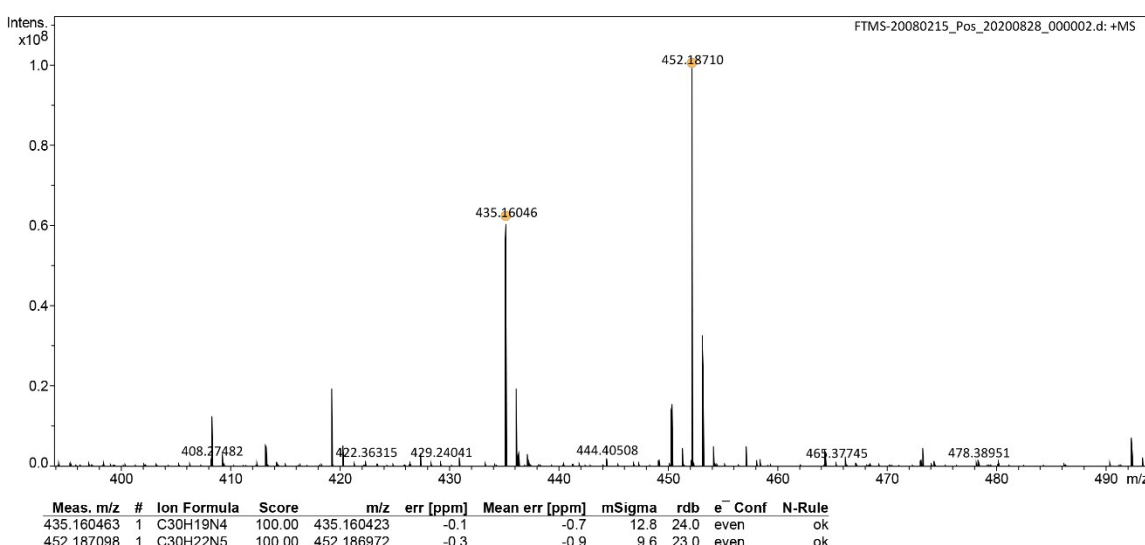


Figure S3. HR-MS spectrum of *p*DCzPyCN.

Nov26-2019. 2. fid
N

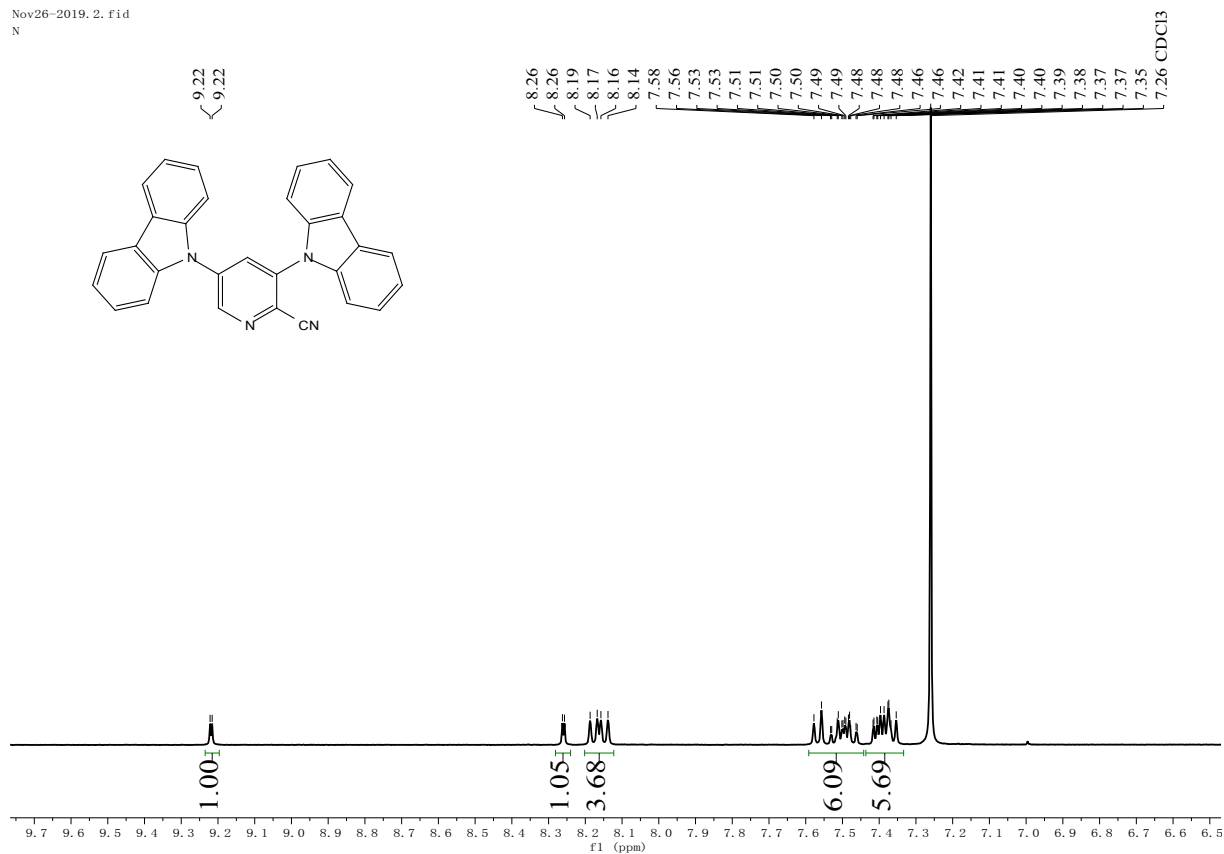


Figure S4. ¹H NMR spectrum of *o*DCzPyCN in CDCl₃.

Aug19-2020.4.fid
P2' C

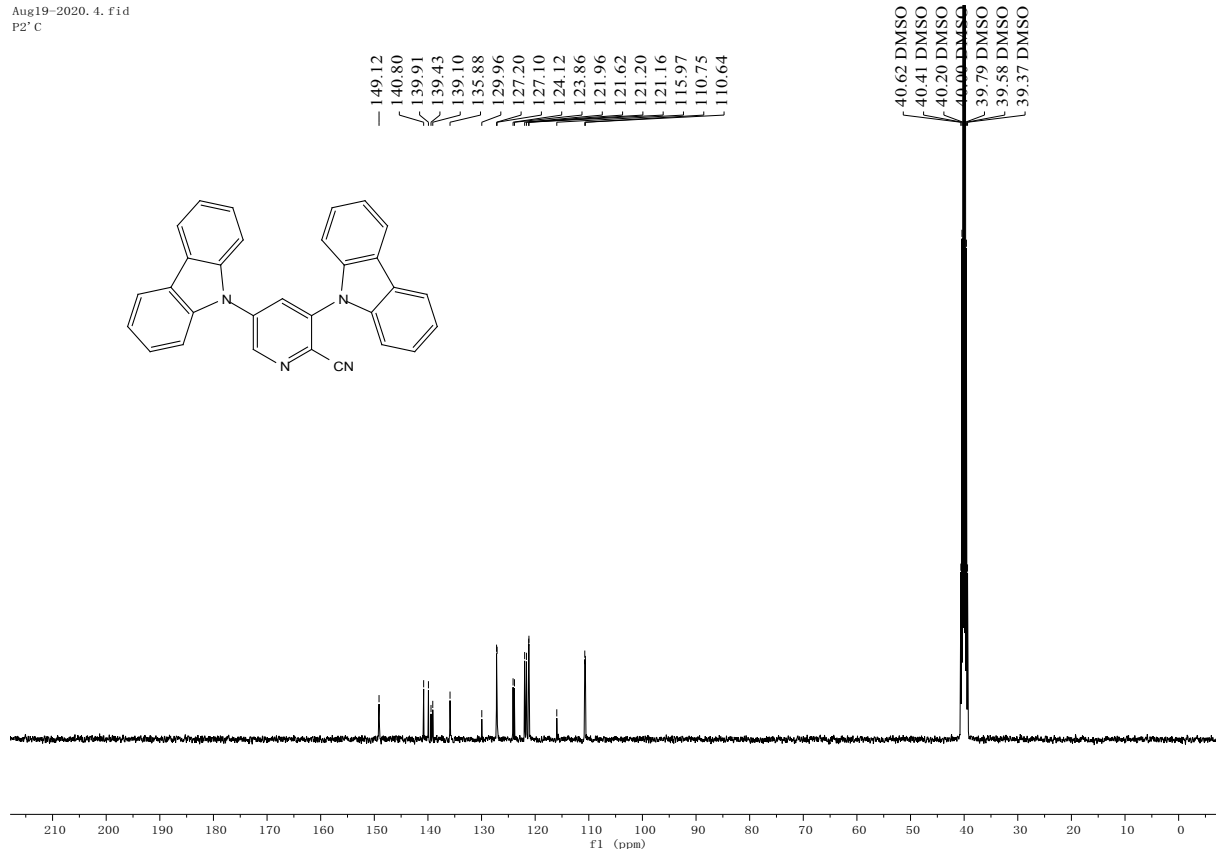


Figure S5. ^{13}C NMR spectrum of *o*DCzPyCN in DMSO.

Peking University Mass Spectrometry Sample Analysis Report

Analysis Info

Analysis Name FTMS-20080215_Pos_20200828_000003.d
Sample oDCzPyCN
Comment

Acquisition Date 8/28/2020 2:34:35 PM
Instrument Bruker Solarix XR FTMS
Operator Peking University

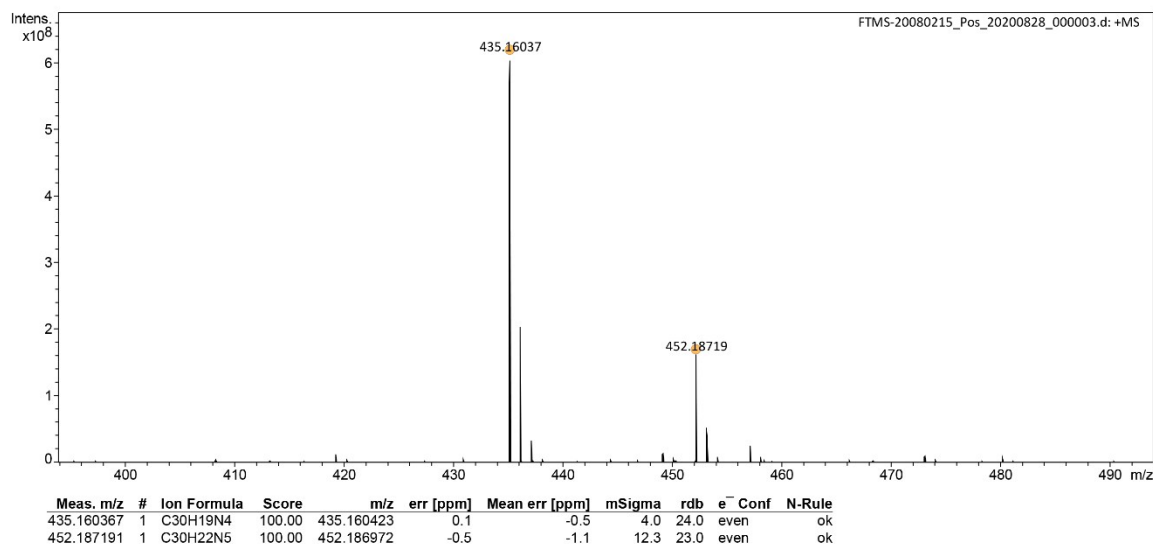


Figure S6. HR-MS spectrum of *o*DCzPyCN.

4. Additional photophysical properties of *p*DCzPyCN, *o*DCzPyCN in solution

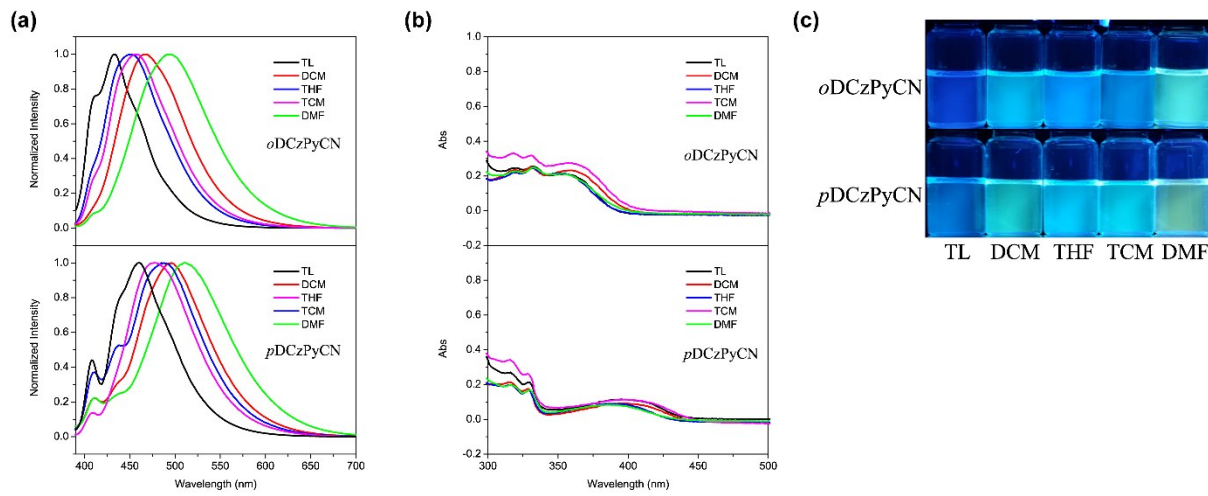


Figure S7. Photophysical properties of *p*DCzPyCN, *o*DCzPyCN in solution. (a) Steady-state photoluminescence and (b) UV absorption spectra of *p*DCzPyCN, *o*DCzPyCN in five types of solvents (toluene(TL), dichloromethane(DCM), tetrahydrofuran(THF), chloroform(TCM),and N,N-Dimethylformamide(DMF)) excited at 365 nm at room temperature. (c) Photographs of *p*DCzPyCN, *o*DCzPyCN in different solution (2.0×10^{-5} M) under 365 nm irradiation.

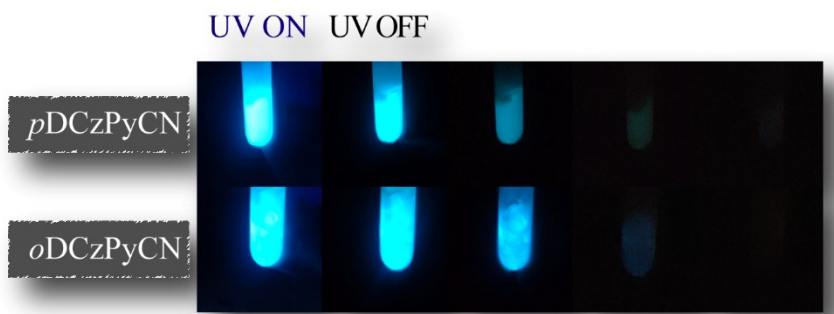


Figure S8. Photographs of *p*DCzPyCN, *o*DCzPyCN in dilute toluene solution (2.0×10^{-5} M) at 77 K before and after excitation light source at 365 nm was switched off.

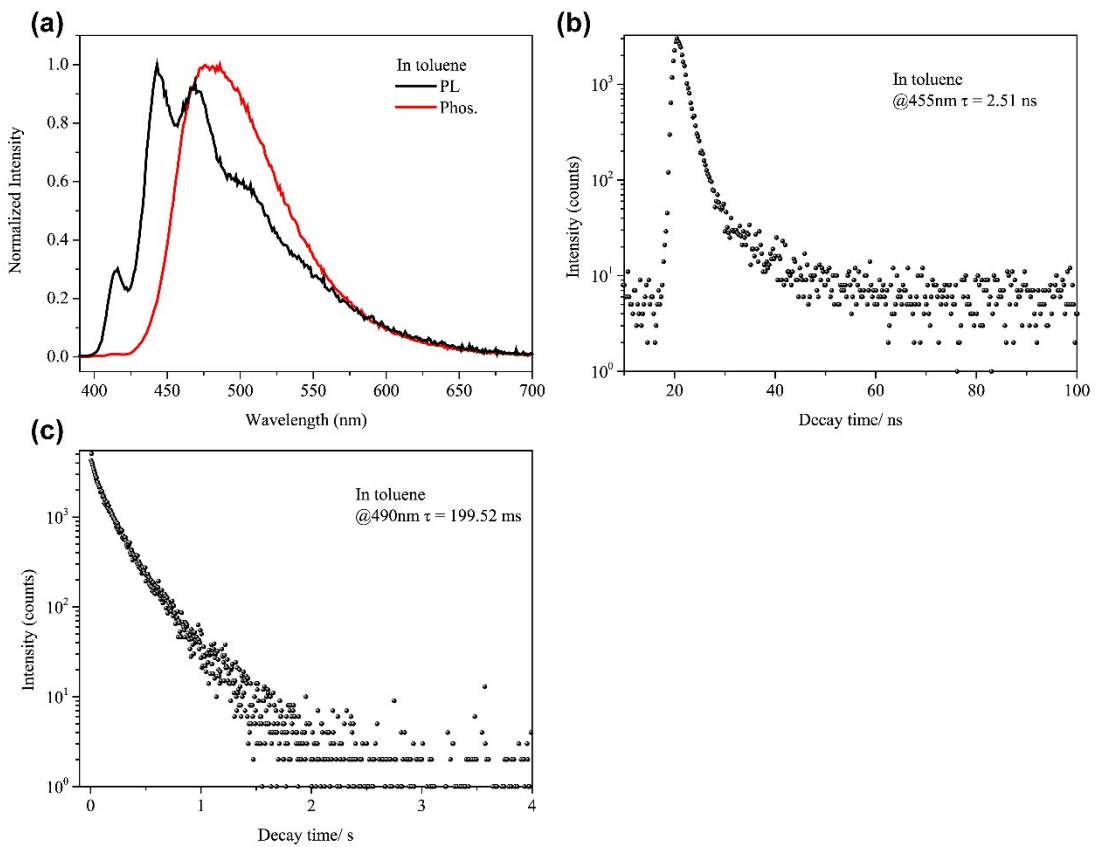


Figure S9. (a) Steady state PL and phosphorescence spectra and (b), (c) the life time decay profiles of **pDCzPyCN** in dilute toluene solution (2.0×10^{-5} M) at 77 K. The excitation wavelength is at 365 nm. The λ_{em} values are listed inside.

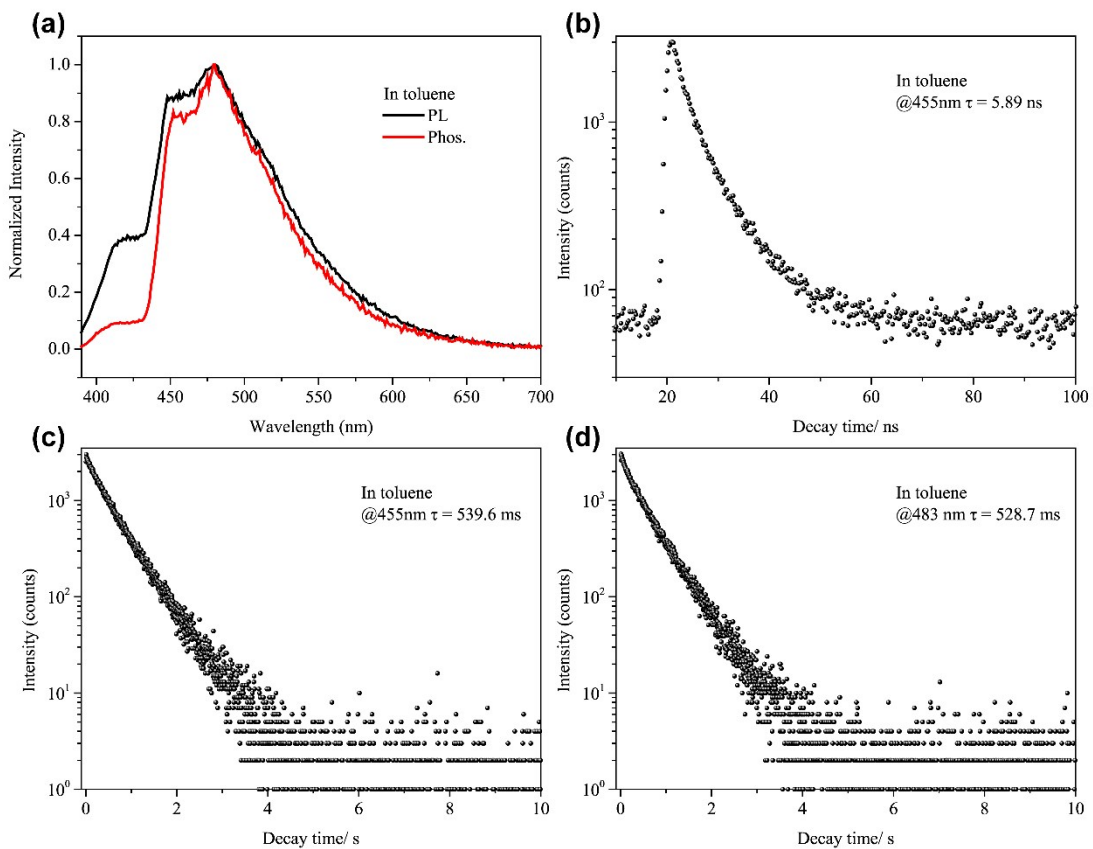


Figure S10. (a) Steady state PL and phosphorescence spectra and (b), (c), (d) the life time decay profiles of *o*DCzPyCN in dilute toluene solution (2.0×10^{-5} M) at 77 K. The excitation wavelength is at 365 nm. The λ_{em} values are listed inside.

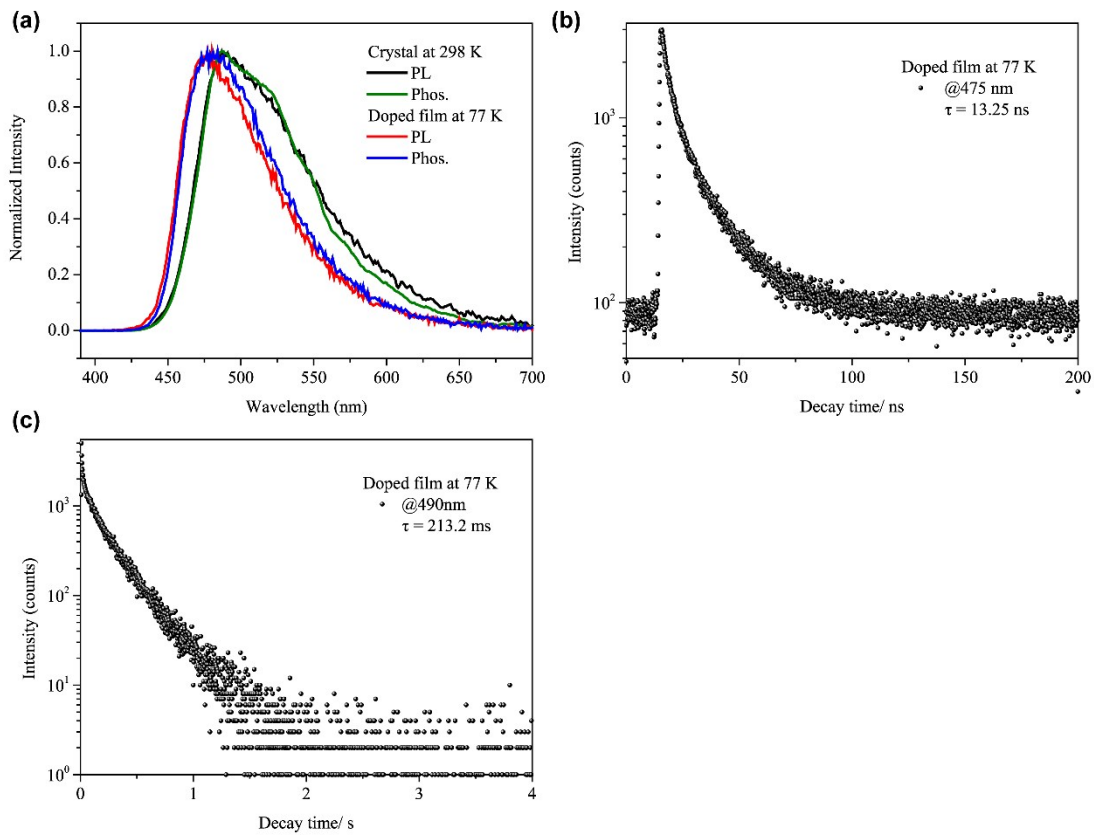


Figure S11. (a) Photoluminescence (black and red curves) and phosphorescence (green and blue curves) spectra of **pDCzPyCN** crystal at 300 K and **pDCzPyCN** (1 wt%)-doped film in polymethyl methacrylate (PMMA) at 77 K. Lifetime decay curves at (b) 475 nm and (c) 490 nm of **pDCzPyCN** (1 wt%)-doped film in PMMA at 77 K.

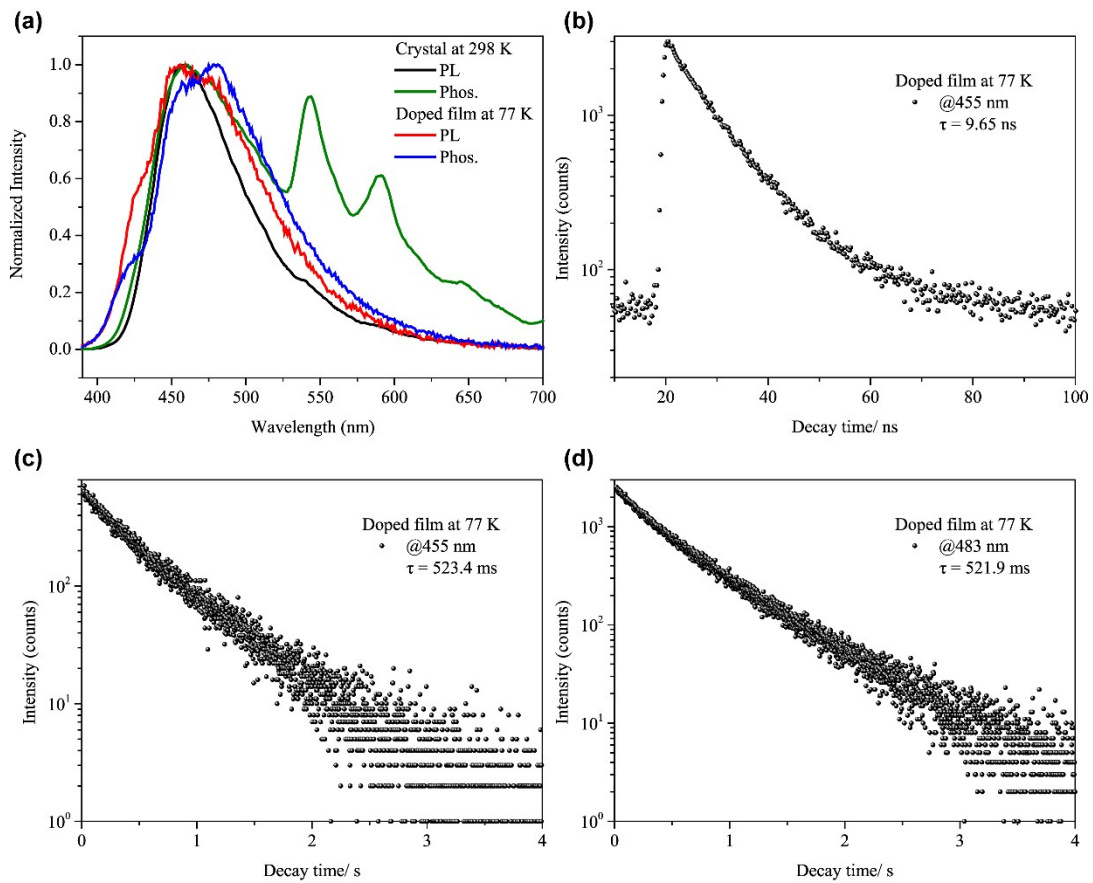


Figure S12. (a) Photoluminescence (black and red curves) and phosphorescence (green and blue curves) spectra of *o*DCzPyCN crystal at 300 K and *o*DCzPyCN (1 wt%)-doped film in polymethyl methacrylate (PMMA) at 77 K. Lifetime decay curves at (b) 455 nm, (c) 455 nm, and (d) 483 nm of *o*DCzPyCN (1 wt%)-doped film in PMMA at 77 K.

Table S1. Photoluminescence lifetime (τ) *p*DCzPyCN, *o*DCzPyCN powders

Compound	Wavelength (nm)	Fluorescence					Phosphorescence				
		τ_1 (ns)	A ₁ (%)	τ_2 (ns)	A ₂ (%)	τ_1 (ms)	A ₁ (%)	τ_2 (ms)	A ₂ (%)	τ_3 (ms)	A ₃ (%)
<i>p</i> DCzPyCN	475	1.65	63.99	13.10	36.01	10.53	20.51	61.67	79.49		
	490					6.57	8.93	35.80	37.76	77.83	53.31
	510					8.19	23.62	58.21	76.38		
	542					8.24	23.90	58.28	76.10		
	592					9.26	21.08	59.77	78.92		
<i>o</i> DCzPyCN	455	3.62	25.33	7.1055	70.66	12.81	8.07	71.49	73.64	193.62	18.29
	542					35.53	6.13	231.59	87.89	629.72	5.98
	592					7.56	1.24	90.43	15.38	293.44	83.38

Table S2. Photoluminescence quantum yield and afterglow efficiency of *p*DCzPyCN, *o*DCzPyCN powders

Compound	$\Phi_{\text{Total}} (\%)$	$\Phi_{\text{Phos}} (\%)$
<i>p</i> DCzPyCN	54.17	36.14
<i>o</i> DCzPyCN	61.60	10.92

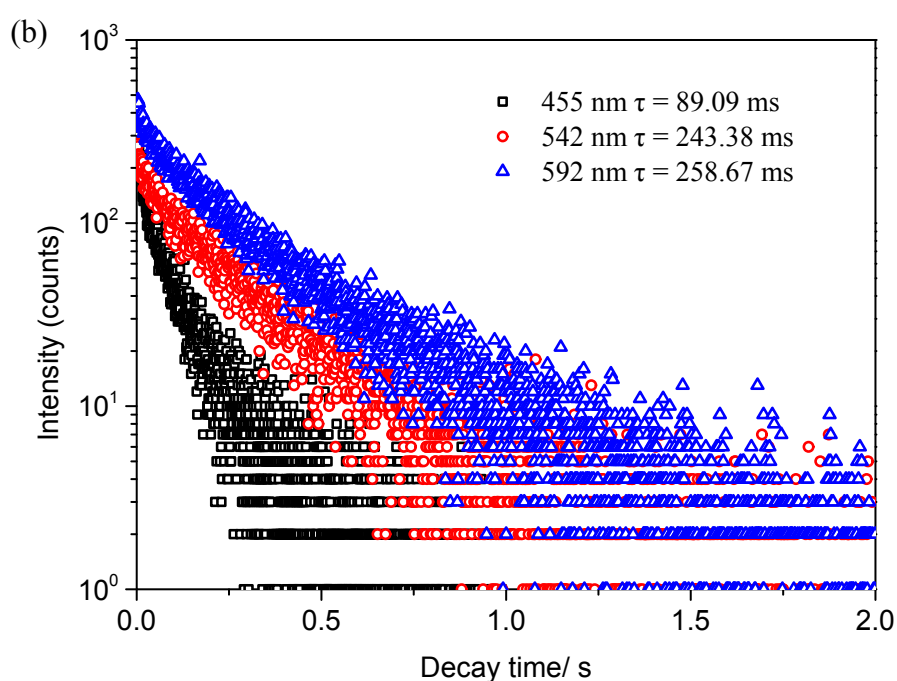
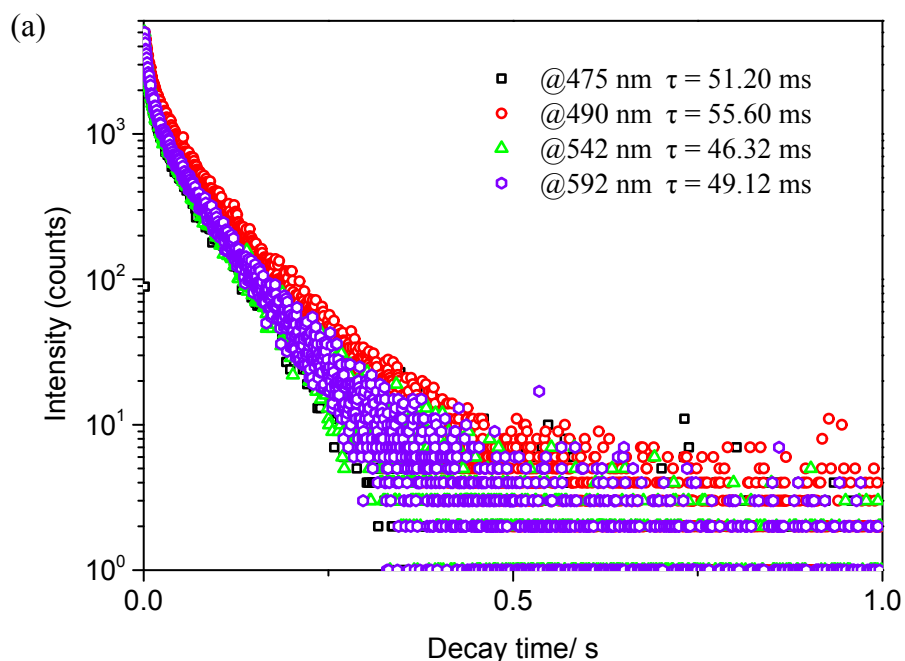


Figure S13. Lifetime decay profiles of the ultralong phosphorescence bands of (a) *p*DCzPyCN, (b) *o*DCzPyCN powders under ambient conditions.

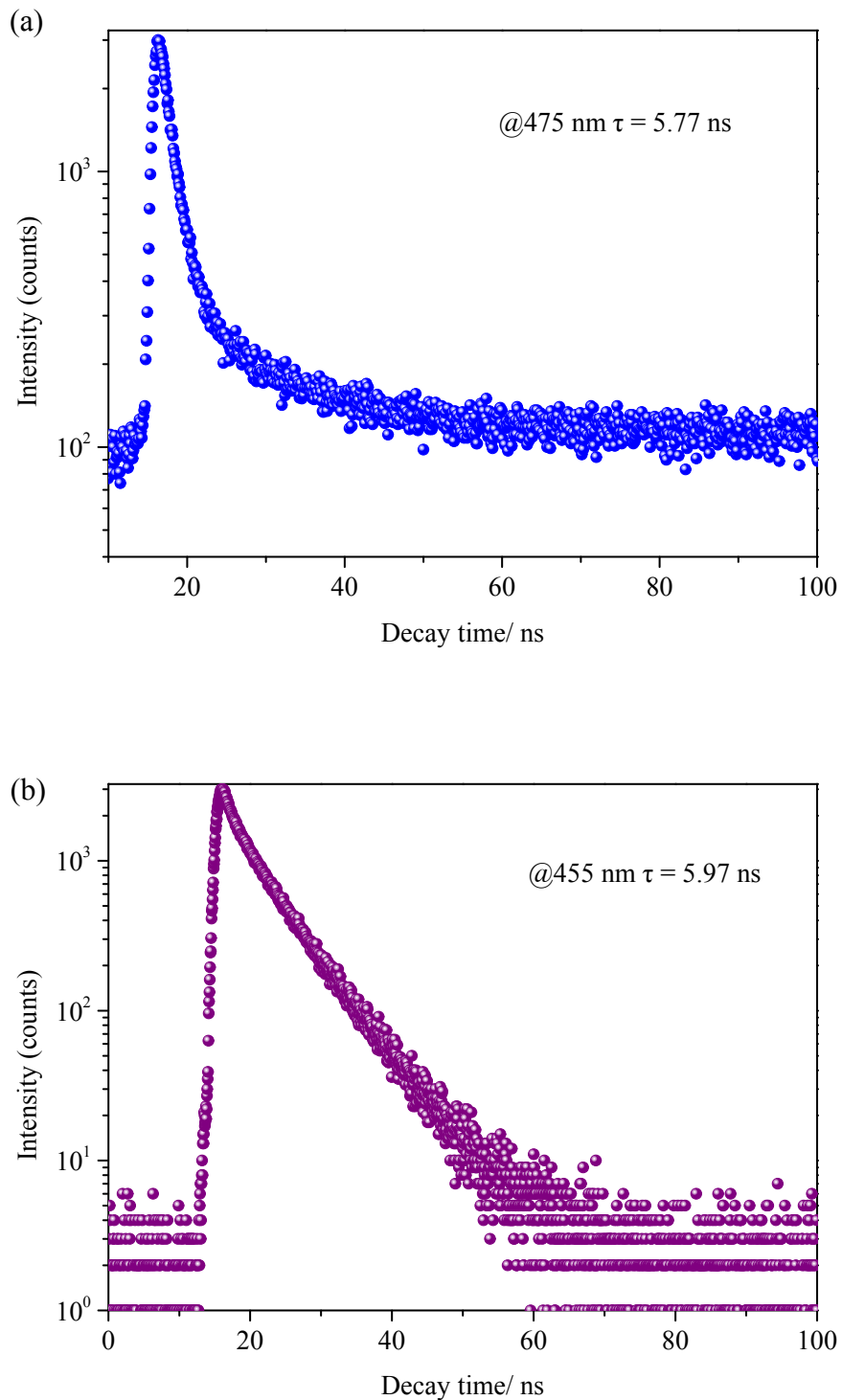


Figure S14. Lifetime decay profiles of the fluorescence emission bands of (a) *p*DCzPyCN, (b)

*o*DCzPyCN powders under ambient conditions.

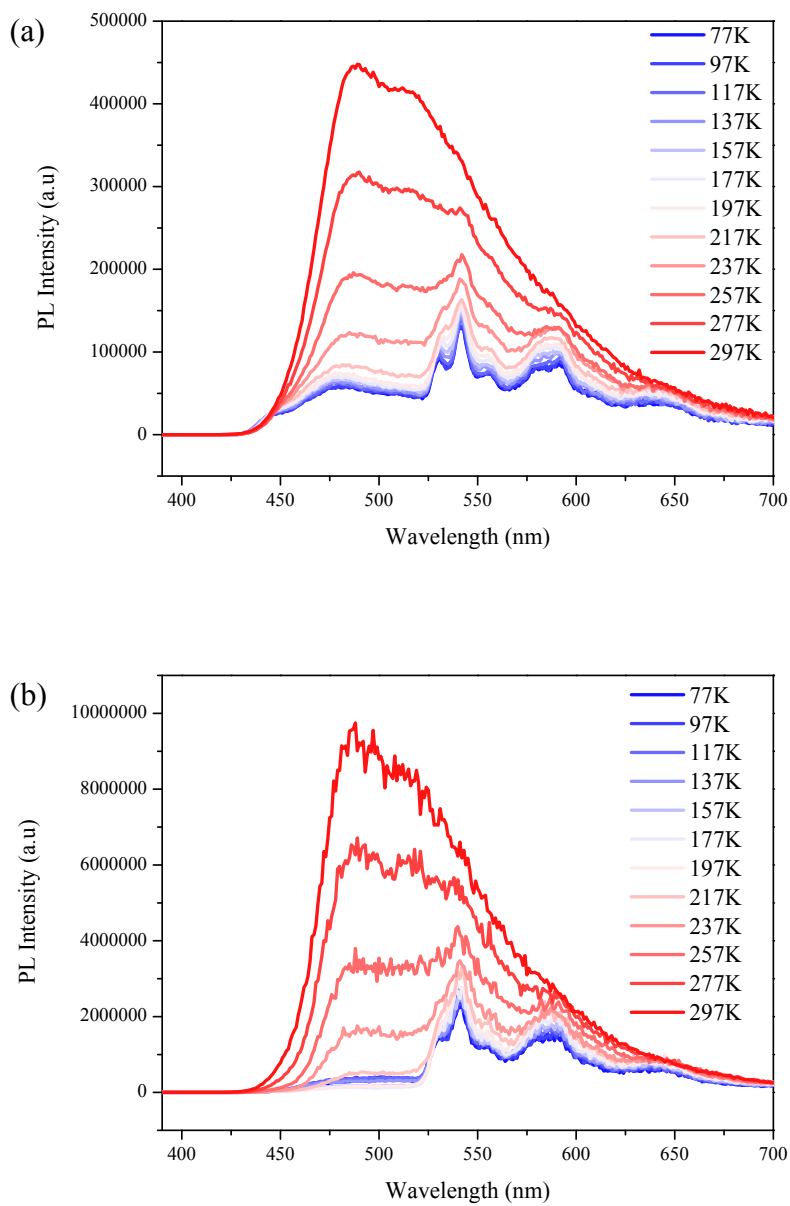


Figure S15. Temperature-dependent steady state PL (a) and phosphorescence (b) spectra of *p*DCzPyCN crystal at different temperatures from 77 K to 297 K. The excitation wavelength is at 365 nm.

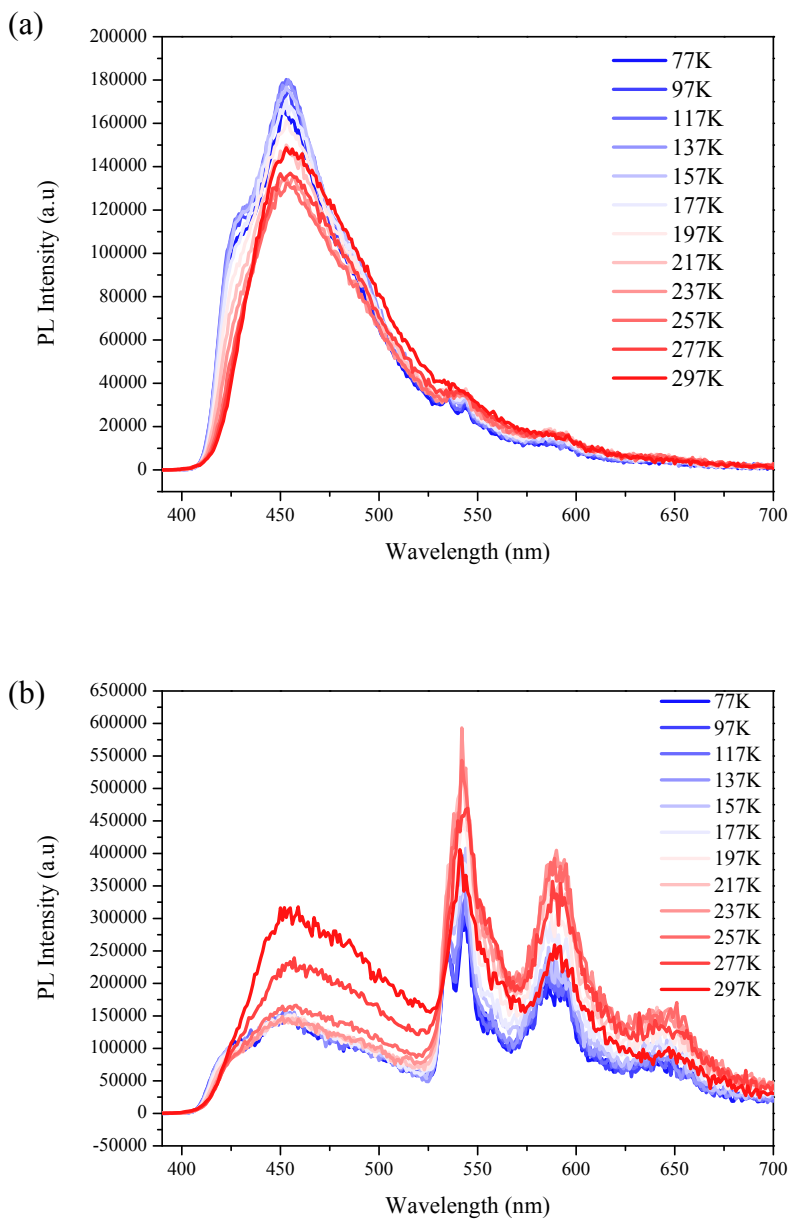


Figure S16. Temperature-dependent steady state PL (a) and phosphorescence (b) spectra of *oDCzPyCN* crystal at different temperatures from 77 K to 297 K. The excitation wavelength is at 365 nm.

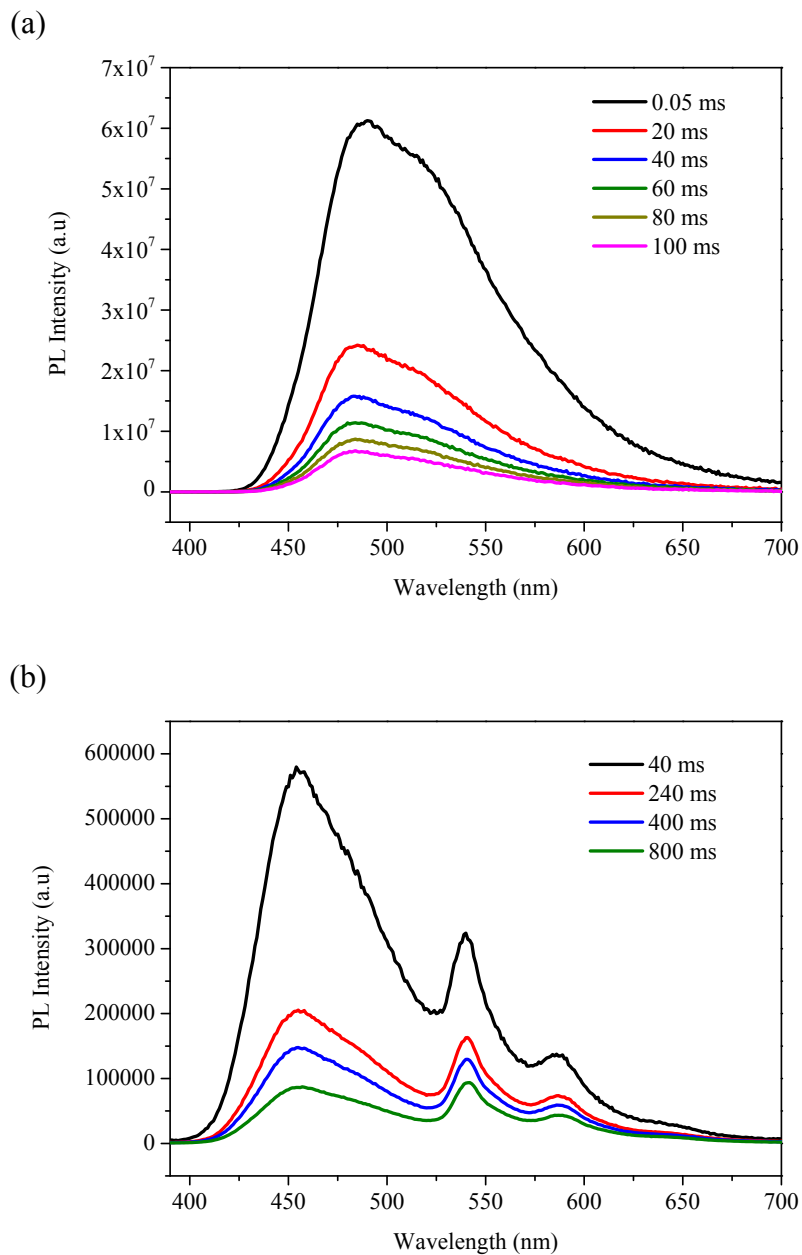


Figure S17. Time-resolved emission spectra with different delay times of *p*DCzPyCN (a) and *o*DCzPyCN (b) at room temperature.

5. Data table of single crystal *p*DCzPyCN, *o*DCzPyCN.

Table S3. Detailed data of *p*DCzPyCN, *o*DCzPyCN single crystals.

Identification code	<i>p</i> DCzPyCN	<i>o</i> DCzPyCN
CCDC Number	2027073	2027075

Empirical formula	C ₃₀ H ₁₈ N ₄	C ₃₀ H ₁₈ N ₄
Formula weight	434.48	434.48
Temperature	110 K	110K
Wavelength	0.71073 Å	0.71073 Å
Crystal system	triclinic	monoclinic
Space group	P-1	C 1 c 1
Unit cell dimensions	a = 5.1918(3) Å, α= 105.516(2)° b = 12.6035(7) Å, β=91.670(2)°. c = 17.9678(10) Å, γ = 100.816(2)°.	a = 16.7453(8) Å, α= 90° b = 13.9681(8) Å, β= 92.658(3)° c = 9.4885(4) Å, γ = 90°
Volume	1108.83(11) Å ³	2216.97(19) Å ³
Z	2	4
Density (calculated)	1.301 Mg/m ³	1.302 Mg/m ³
Absorption coefficient	0.078 mm ⁻¹	0.078 mm ⁻¹
F(000)	452	904
Theta range for data collection	6.48 to 51.98°.	6.16 to 52°.
Index ranges	-17≤h≤30, -28≤k≤30, -10≤l≤18	-10≤h≤10, -12≤k≤11, -16≤l≤17
Reflections collected	12348	9005
Independent reflections	4441[R(int) =0.0357]	4315[R(int) =0.0271]
Final R indices	R1 = 0.0444, wR2 = 0.0922 [I>2sigma(I)]	R1 = 0.0395, wR2 = 0.0874
R indices (all data)	R1 = 0.0612, wR2 = 0.1005	R1 = 0.0496, wR2 = 0.0941

6. Unit cell in the single crystal of *p*DCzPyCN, *o*DCzPyCN

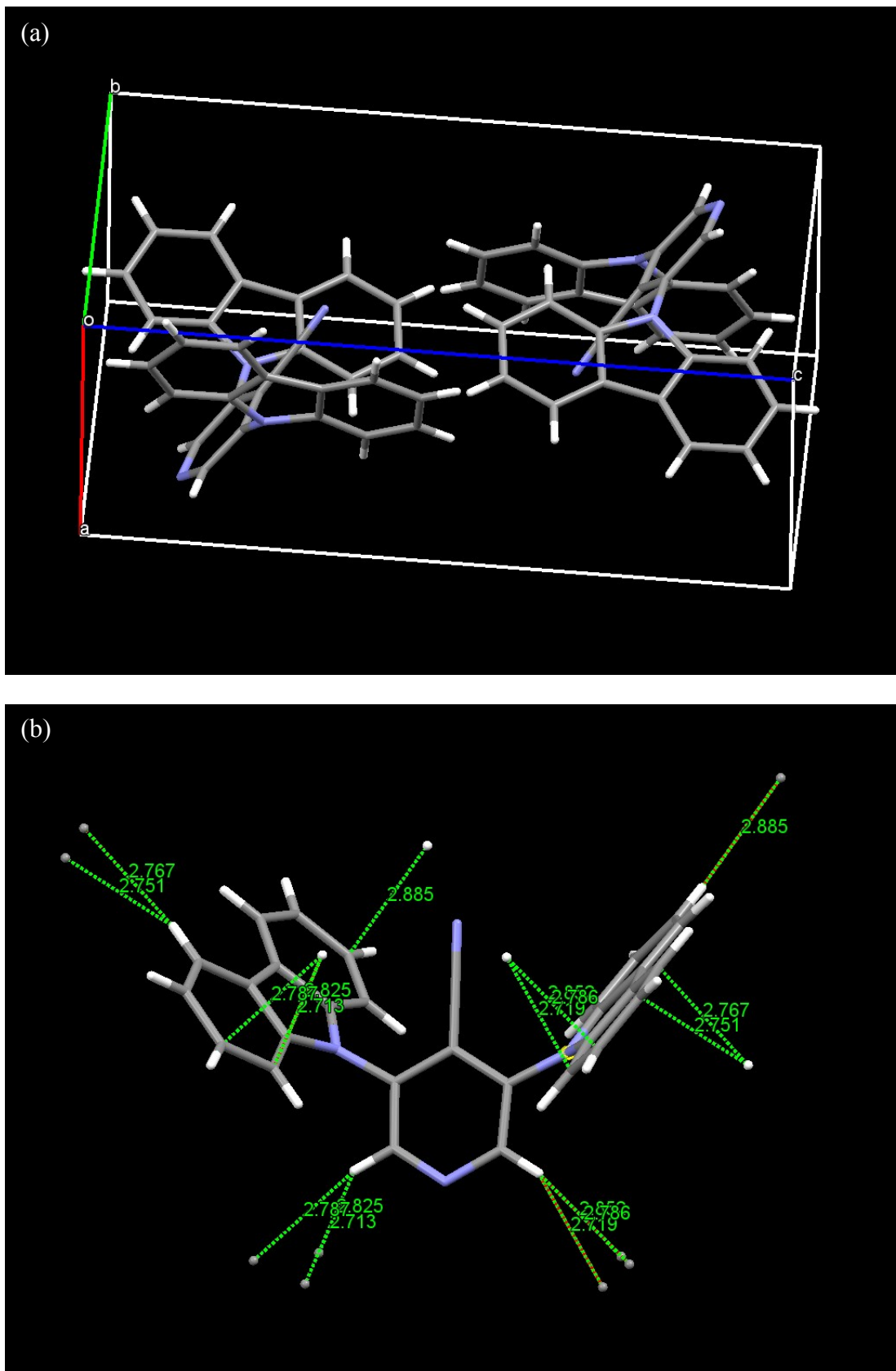
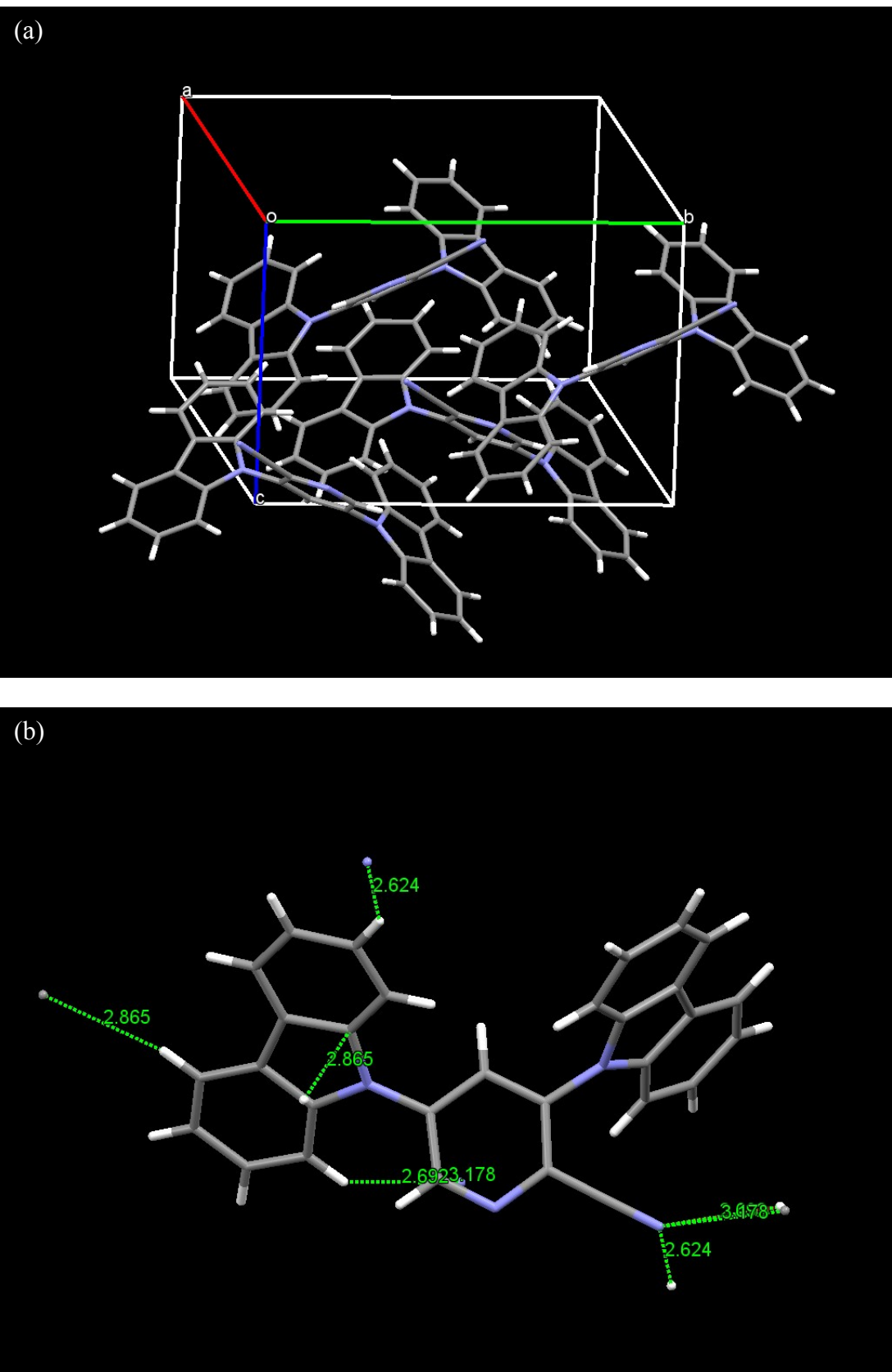


Figure S18. (a) The steric unit cell of *p*DCzPyCN; (b) the intermolecular interactions between adjacent molecules.



7. TD-DFT results

Table S4. Triplet excited states of *p*DCzPyCN containing the same orbital transition components of S1.

Excited State	Energy (eV)	Transition configuration (%)
Monomer		
T1	2.5805	H→L(97.3%)
T2	2.6745	H-10→L(2.2%), H-1→L(92.8%)
S1	2.6990	H→L(99.5%)
Dimer		
T1	2.5327	H-4→L(41.6%), H-2→L (39.5%), H→L(14.5%)
T2	2.5785	H-4→L(7.3%), H-2→L (7.5%), H→L(62.8%), H→L+1(20.9%)
S1	2.5954	H-4→L(2.6%), H-2→L (2.6%), H→L (91.4%), H→L+1(3.1%)
T3	2.6245	H-5→L(67.0%), H-3→L (11.2%), H-1→L(13.7%)
T4	2.6871	H-5→L(11.2%), H-1→L (54.0%), H-1→L+1(28.3%)
T5	2.7214	H→L(22.3%), H→L+1(73.9%)
T6	2.8210	H-1→L(30.7%), H-1→L+1(61.2%)

Table S5. Triplet excited states of *o*DCzPyCN containing the same orbital transition components of S1.

Excited State	Energy (eV)	Transition configuration (%)
Monomer		
T1	2.8005	H-7→L(2.9%), H-6→L (3.6%), H-2→L(24.3%), H-1→L(34.9%), H→L(27.6%)
T2	2.9441	H-2→L(8.0%), H-1→L (18.2%), H→L(68.9%)
S1	3.0103	H→L(97.9%)
T3	3.1565	H-4→L+3(3.1%), H-2→L+3 (43.6%), H-1→L(2.5%), H-1→L+3(27.0%), H→L+1(4.4%), H→L+3(2.4%), H→L+5(6.6%)
T4	3.1856	H-5→L+2(3.23%), H-3→L (7.8%), H-3→L+2(68.4%), H-2→L+4(3.1%), H-1→L+4(4.5%)
T5	3.2179	H-6→L+1(2.0%), H-2→L (2.9%), H-2→L+1(2.9%), H-2→L+3(2.1%), H-1→L+1(2.7%), H-1→L+3(2.7%), H→L+1(74.2%)
Dimer		
T1	2.7238	H-16→L(2.1%), H-5→L (34.4%), H-4→L(16.8%), H-3→L(2.1%), H-2→L(20.2%), H-1→L(13.0%), H→L(2.7%)

T2	2.8683	H-5→L(17.1%), H-4→L (13.6%), H-3→L(3.1%), H-2→L(58.1%)
T3	2.8688	H-12→L+1(5.0%), H-12→L+2 (2.2%), H-1→L+1(4.9%), H-1→L+2(2.1%), H→L+1(53.2%), H→L+2(21.9%)
S1	2.9155	H-3→L(4.5%), H-2→L(65.8%), H-1→L(18.6%), H→L(8.9%)
T4	2.9791	H-5→L(2.1%), H-2→L (5.9%), H-1→L(11.3%), H→L(77.8%)
T5	3.0529	H-2→L(6.0%), H-1→L(70.90%), H→L(17.9%)
T6	3.1256	H-6→L(4.4%), H-6→L+5(4.1%), H-6→L+7(8.4%), H-3→L(42.5%), H-3→L+5(19.7%), H-3→L+7(2.3%), H-2→L+9(2.3%)
T7	3.1633	H-7→L+3(2.6%), H-5→L+6(10.1%), H-4→L(4.4%), H-4→L+5(3.1%), H-4→L+6(22.7%), H-3→L(10.7%), H-3→L+5(2.5%), H-2→L+1(2.0%), H-2→L+2(7.4%), H-1→L+1(4.0%), H-1→L+11(2.4%)
T8	3.1683	H-7→L+3(3.8%), H-6→L+7(2.2%), H-5→L+6(8.2%), H-4→L+5(2.6%), H-4→L+6(15.8%), H-3→L(14.2%), H-3→L+5(5.5%), H-2→L+1(6.3%), H-2→L+2(10.2%), H-1→L+2(3.6%), H-1→L+11(2.1%)
T9	3.1719	H-7→L(6.1%), H-7→L+3(25.7%), H-6→L+7(7.6%), H-5→L+8(2.0%), H-3→L(11.0%), H-3→L+5(9.7%), H-3→L+6(2.0%), H-2→L+1(2.7%), H-2→L+2(2.1%), H-2→L+5(2.7%)
T10	3.1762	H-7→L(6.5%), H-7→L+3(26.7%), H-6→L+5(4.6%), H-6→L+7(3.1%), H-5→L+8(2.0%), H-3→L+2(2.6%), H-3→L+7(8.2%), H-2→L+1(6.8%), H-2→L+2(7.5%), H-2→L+5(3.0%)
T11	3.1856	H-6→L+5(18.0%), H-6→L+6(2.1%), H-3→L(7.9%), H-3→L+5(2.7%), H-3→L+7(19.3%), H-2→L+1(4.0%), H-2→L+2(13.1%), H-2→L+7(3.6%)

8. Diagrams of the TD-DFT calculated energy levels of *p*DCzPyCN, *o*DCzPyCN

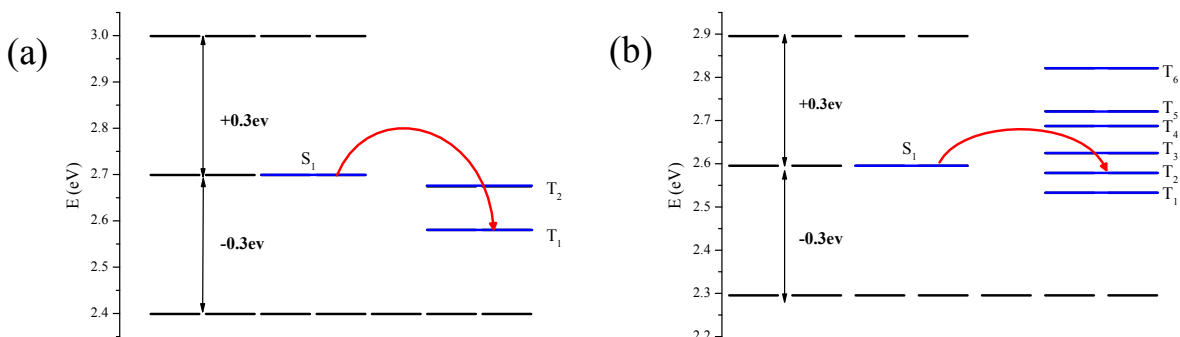


Figure S20. Diagrams of the TD-DFT calculated energy levels and possible ISC channels of *p*DCzPyCN monomer (a), dimer (b) at the singlet (S_1) and triplet (T_n) states.

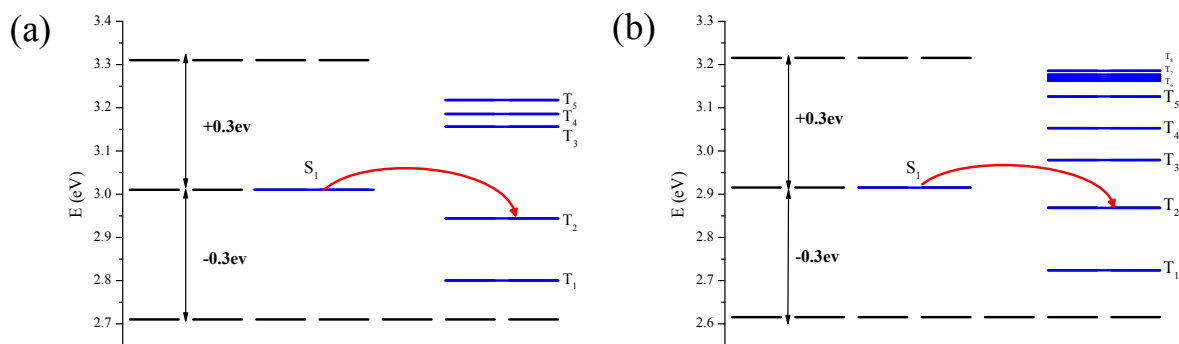


Figure S21. Diagrams of the TD-DFT calculated energy levels and possible ISC channels of *o*DCzPyCN monomer (a), dimer (b) at the singlet (S_1) and triplet (T_n) states.

References:

- [1] L. Jian - An, Z. Jinghong, M. Zhu, X. Zongliang, Y. Zhan, X. Bingjia, L. Cong, C. Xin, R. Dingyang, P. Hui, S. Guang, Z. Yi, C. Zhenguo, *Angew. Chem. Int. Ed.* **2018**, *57*, 6449-6453.
- [2] Z. An, C. Zheng, Y. Tao, R. Chen, H. Shi, T. Chen, Z. Wang, H. Li, R. Deng, X. Liu, W. Huang, *Nat. Mater.* **2015**, *14*, 685-690.